JB
Journals.ASM.org

Cell Growth Inhibition upon Deletion of Four Toxin-Antitoxin Loci from the Megaplasmids of *Sinorhizobium meliloti*

Branislava Milunovic, George C. diCenzo, Richard A. Morton, Turlough M. Finan

Center for Environmental Genomics, Department of Biology, McMaster University, Hamilton, Ontario, Canada

Toxin and antitoxin (TA) gene pairs are addiction systems that are present in many microbial genomes. *Sinorhizobium meliloti* is an N_2-fixing bacterial symbiont of alfalfa and other leguminous plants, and its genome consists of three large replicons, a circular chromosome (3.7 Mb) and the megaplasmids pSymA (1.4 Mb) and pSymB (1.7 Mb). *S. meliloti* carries 211 predicted type II TA genes, each encoding a toxin or an antitoxin. We constructed defined deletion strains that collectively removed the entire pSymA and pSymB megaplasmids except for their *oriV* regions. Of approximately 100 TA genes on pSymA and pSymB, we identified four whose loss was associated with cell death or stasis unless copies of the genes were supplied in *trans*. Orthologs of three of these loci have been characterized in other organisms (*relB/E* [*sma0471/sma0473*], *Fic* [*DOC*] [*sma2105*], and *VapC* [*PIN*] [*orf2230/sma2231*]), and this report contains the first experimental proof that *RES/Xre* (*smb21127/smb21128*) loci can function as a TA system. Transcriptome sequencing (RNA-seq) analysis did not reveal transcriptional differences between the TA systems to account for why deletion of the four "active" systems resulted in cell toxicity. These data suggest that severe cell growth phenotypes result from the loss of a few TA systems and that loss of most TA systems may result in more subtle phenotypes. These four TA systems do not appear to play a direct role in the *S. meliloti*-alfalfa symbiosis, as strains lacking these TA systems had a symbiotic N_2 fixation phenotype that was indistinguishable from the wild type.

Toxin (T) and antitoxin (A) genes are ubiquitous and somewhat mysterious with respect to function. Type II TA systems are those in which the antitoxin and toxin are both proteins, and these are generally transcribed as antitoxin-toxin gene pairs (1–3). During unperturbed, exponential growth, the toxic activity of the toxin is neutralized through a physical interaction with the antitoxin protein, and in most systems, the TA protein complex also regulates TA transcription by binding to the TA promoter region (3).

Under conditions where the number of toxin molecules is greater than those of the antitoxin, the toxin is free to exert its effect on the cell. Several mechanisms lead to conditions where the toxin molecules outnumber the antitoxin molecules. When a TA pair is lost from the cell, the residual antitoxin degrades faster than the toxin (2, 4). Alternatively, the antitoxins can be degraded by Lon or Clp proteases (2, 5, 6). The loss of the antitoxin releases the toxin, which subsequently interferes with a vital cell process (2, 3, 7). Some toxins insert into and destabilize the membrane, others interact with DNA gyrase and interfere with DNA replication, and others disrupt translation either by functioning as an endoribonuclease or through an interaction with the ribosome (8–10).

Why TA systems are maintained within the genome is an area of active research, and many hypotheses have been put forth (7, 11). The simplest of these models suggest that they are involved in stabilizing plasmids and nonessential chromosomal segments, or possibly that they function as plasmid antiaddiction modules (12, 13). An alternative hypothesis is that they are abortive infection systems involved in a population-level defense against phage infection (14). Other models postulate that TA systems are involved in the metabolic regulation of the cell or help the cell adapt to various stresses via persister cell formation (15–17). Here, we report a deletion analysis of the megaplasmids of the alphaproteobacterium *Sinorhizobium meliloti* and we focus on how the loss of TA genes affects cell growth. *S. meliloti* has a multipartite genome, and it lives both as a free-living soil bacterium and in a symbiosis within N_2-fixing root nodules on plants such as alfalfa (*Medicago sativa*) and sweet clover (*Melilotus alba*). The model *S. meliloti* strain, 1021, contains a circular chromosome (3.7 Mb) and two megaplasmids, pSymA (1.4 Mb) and pSymB (1.7 Mb) (18–20). Surveys of worldwide isolates show that the presence of two very large megaplasmids and a circular chromosome is a feature of the *S. meliloti* genome. The megaplasmids are notable for their essential role in establishing a successful symbiosis with host plants (19–23). The replicons also appear valuable for free-living growth as they carry loci that increase metabolic diversity, such as a denitrification pathway on pSymA (19, 24, 25), a high density of solute transport systems on pSymB (20, 26, 27), and genes involved in osmoadaptation on pSymB (28). Two essential genes, *engA* and the only copy of an Arg-tRNA gene, are located on pSymB, and there is strong evidence that the DNA region containing these genes translocated from the chromosome to pSymB in an ancestral strain (29). Megaplasmid pSymA is a nonessential replicon (30). Yurgel et al. (31) recently reported on a collection of 50 SymA deletion derivatives and identified loci involved in cytochrome *c* activity, growth on various carbon and nitrogen sources, and symbiotic N_2 fixation effectiveness.

Outside the above-mentioned processes, relatively few functions have been attributed to the *S. meliloti* megaplasmids, despite their carrying almost 2,900 predicted protein-coding genes (19, 20). Bioinformatics studies suggest that about 100 megaplasmid

Received 18 September 2013 **Accepted** 27 November 2013
Published ahead of print 6 December 2013
Address correspondence to Turlough M. Finan, finan@mcmaster.ca.
Supplemental material for this article may be found at http://dx.doi.org/10.1128/JB.01104-13.

doi:10.1128/JB.01104-13

genes (>3% of the predicted genes) encode toxin or antitoxin proteins (1, 32). Here, we describe the construction of a deletion library that spans both the pSymA and pSymB megaplasmids except for the regions directly surrounding the *oriV*s. We show that of the ~100 TA genes deleted, loss of only four TA loci was associated with subsequent cell death or stasis. Examination of transcription of the TA genes by transcriptome sequencing (RNA-seq) analysis revealed no correlation between the expression of the TA loci and their growth phenotype. To our knowledge, this work represents the largest systematic deletion analysis of TA genes reported to date.

MATERIALS AND METHODS

Bacterial strains and plasmids. Bacterial strains and plasmids are listed in Table S1 in the supplemental material. All the *S. meliloti* strains are derived from the 1021 derivative, RmP110, which carries a functional *pstC* gene (33).

Medium, antibiotics, and growth conditions. Luria-Bertani (LB) medium contained 10 g Difco tryptone, 5 g Difco yeast extract, and 5 g NaCl per liter of H_2O. For *S. meliloti*, LB was supplemented with 2.5 mM $MgSO_4$ and 2.5 mM $CaCl_2$ (LBmc). Minimal medium M9 contained, per liter, 5.8 g Na_2HPO_4, 3 g KH_2PO_4, 0.5 g NaCl, 1 g NH_4Cl, 1 μg/ml biotin, 10 ng/ml $CoCl_2$, 1 mM $MgSO_4$, 0.25 mM $CaCl_2$, and 10 mM carbon source. For screening compounds as sources of nitrogen, NH_4Cl was omitted from M9. Antibiotic (streptomycin [Sm], neomycin [Nm], spectinomycin [Sp], gentamicin [Gm], tetracycline [Tc], and chloramphenicol [Cm]) concentrations in liquid and solid media were as previously described (34, 35). In liquid medium, the antibiotic concentrations were halved. X-Gal (5-bromo-4-chloro-3-indolyl-β-D-galactopyranoside) and IPTG (isopropyl-β-D-thiogalactopyranoside) were used at the final concentrations of 40 μg/ml and 0.5 mM, respectively. *S. meliloti* strains were grown at 30°C while *Escherichia coli* strains were grown at 37°C.

DNA manipulations. Genomic DNA from *S. meliloti* and plasmid DNA from *E. coli* were isolated as previously described (36). Agarose gel electrophoresis and other recombinant DNA techniques such as restriction analysis and DNA ligation and transformation were done according to reference 36. DNA sequencing was performed by the MOBIX facility at McMaster University, Hamilton, Ontario, Canada.

FRT targeting vector pTH1937. Plasmid pTH1937 carries the p15A *oriV* from pACYC177 (37); the *nptII* gene (neomycin resistance) from Tn*5*; a multiple cloning site (MCS) containing the unique restriction sites SpeI, SwaI, EcoRV, PvuI, PacI, and EcoRI; the *oriT* from RK2; and an FLP recombination target (FRT) site. pTH1937 was targeted to specific locations in the *S. meliloti* genome, by amplifying DNA as SpeI-EcoRI fragments from the pTH1522 *S. meliloti* genomic library (35) into the SpeI-EcoRI sites in pTH1937. All constructs were confirmed by DNA sequencing.

Plasmid pTH1937 was made as follows: the multiple cloning site (MCS) was generated by annealing the complementary oligonucleotides 49 and 57 bp long into an EcoRI/SphI-digested PCR product from pACYC177 (amplified with the primers ML7057 [AC**GAATTC**CTGTCA GACCAAGTTTACTC] and ML7058 [TG**GCATGC**TGAATACTCATAC TCTTCC]) spanning nucleotides (nt) 618 to 3709 to give plasmid pTH1998. A SphI/BglII 109-bp FRT fragment from pMS101 (38) was cloned into pTH1998 to form pTH1999. The Tn*903* inverted repeat in pTH1999 was excised by digestion with NheI and DraIII, and the recessed 3′ termini were filled in (Klenow DNA polymerase [pol]) and ligated to give pTH2000. A 2.2-kb product from nt 2735 to 1951 of pTH2000 was PCR amplified (ML9318 [CATG**CCATGG**TTTTCGCACGATATAC AGG] and ML9319 [CTA**GCTAGC**TGATAGGTGGGCTGCCCTTC]) and ligated to a 267-bp NcoI/NheI fragment containing the *oriT* site from pRK2 to give plasmid pTH2001 (restriction sites are shown in bold). A 1.5-kb PCR product with SmaI and XhoI sites from nt 1898 to 980 of pTH2001 was PCR amplified (ML9647 [CCG**CTCGAG**CGGTATCTGG ACAAGGGAAAACG] and ML9648 [TCC**CCCGGG**GGACTCAGAAGA ACTCGTCAAG]) and ligated with the *nptII* gene (neomycin resistance) from Tn*5* (1,036-bp SmaI/XhoI fragment amplified from pTH1360) to produce the plasmid pTH1937.

Construction of *S. meliloti* strains carrying two FRT sites. Previously, an *S. meliloti* RmP110 gene fusion library was constructed through single crossover recombination of pTH1522 into the genome (35). The pTH1522 vector carries an FRT site, and the location of the insertion was previously determined through sequencing. The pTH1522 library strains were used as recipients for a triparental mating with an *E. coli* strain carrying pTH1937 (FRT, Nm^r) with the appropriate *S. meliloti* DNA fragment. Plasmids were mobilized from *E. coli* to *S. meliloti* in triparental matings with the *E. coli* MT616 strain carrying pRK600 (23).

Construction of the *flp* delivery vector pTH1944. Plasmid pTH1944 was constructed in order to express *flp* recombinase in *S. meliloti*. A 2-kb PstI fragment containing the *flp* gene from pTH472 (40) was cloned into pTH1919 (J. Cheng and T. Finan, unpublished data) to produce pTH1944. In pTH1944, *flp* is transcribed from the *lac* promoter (nt 4088 to 4127) and *lac* operator (*lacO*) sites are present at nt 4068 to 4091. While pTH1944 does not carry the *lacI* gene, in some experiments $lacI^q$ was expressed from the pTH1931 plasmid (29) and *flp* expression was induced by adding 0.5 mM IPTG to the medium. *S. meliloti* strain RmH940 contains a *lacZ-nptII* (Nm^r) cassette flanked by FRT sites in direct orientation (40). In control experiments, pTH1944 resulted in 100% excision of the FRT-flanked *lacZ-nptII* genes in *S. meliloti* RmH940 when 0.5 mM IPTG was present in the medium. In the absence of IPTG, 90% of the RmH940 transconjugants retained the FRT-flanked *lacZ-nptII* genes.

Megaplasmid deletions. The majority of the deletions in this study were made via transfer of the Flp recombinase plasmid pTH1944 (Tc^r) into the *S. meliloti* ΦpTH1522ΦpTH1937 double integrant strains (transfer frequency, 10^{-4}/recipient). However, several additional deletions were made by combining two individual FRT-marked deletions by transduction of Gm^r Nm^r-marked deletions into recipient FRT-deletion strains that lacked antibiotic resistance markers (see Fig. 1). Prior to these transductions, it was essential to cure the Tc^r pTH1944 *flp* plasmid from the recipient cells, and this was done by sequential subculturing and screening for Tc^s colonies. Strains carrying FRT-flanked regions A150, A152, and A160 were generated as follows: A150 [ΦΔA127 (Gm^r Nm^r) → ΔA106] (nt 186200 to 930000), A152 [ΦΔA129 (Gm^r Nm^r) → ΔA117] (nt 402136 to 1122176), and A160 [ΦΔA105 (Gm^r Nm^r) → ΔA102] (nt 10988 to 184519). Subsequent deletion of the regions between the FRT sites was achieved upon conjugation of the *flp* (pTH1944-Tc^r) plasmid into these strains, and the deletions ΔA150, ΔA152, and ΔA160 were generated. ΔB180 was constructed by transducing ΔB143 (nt 635940 to 678812) into ΔB139 (nt 740722 to 869642) without first curing pTH1944.

Cloning toxin-antitoxin gene regions. DNA fragments containing the *sma0471/sma0473*, *sma2151*, *sma2231*, *sma2253/sma2255*, *sma2273/sma2275*, and *sma2105* genes; the upstream region of *sma2105*; the *sma2133* and *smb21127/smb21128* genes; and their predicted promoter regions were amplified from RmP110 DNA using the primers listed in Table S2 in the supplemental material. The products were cloned as a PacI fragment into the Sp^r broad-host-range expression vector pTH1931 to produce plasmids pTH2563, pTH2622, pTH2623, pTH2624, pTH2625, pTH2646, pTH2790, pTH2647, and pTH2830, respectively.

Growth curves and viable cell counts. Cultures were grown and aerated on a roller drum (Rollordrum; New Brunswick Scientific Co., Edison, NJ, USA) at 30°C. Strains grown overnight in LBmc medium were subcultured to an optical density at 600 nm (OD_{600}) of 0.03 to 0.04 in 5 ml LBmc with or without IPTG (0.5 mM). Growth was measured by monitoring the OD_{600} of the culture every 3 h. The number of CFU was determined by plating samples on LB medium with or without IPTG (cultures without IPTG were plated on plates without IPTG and cultures with IPTG were plated on plates with IPTG, except for the zero time point).

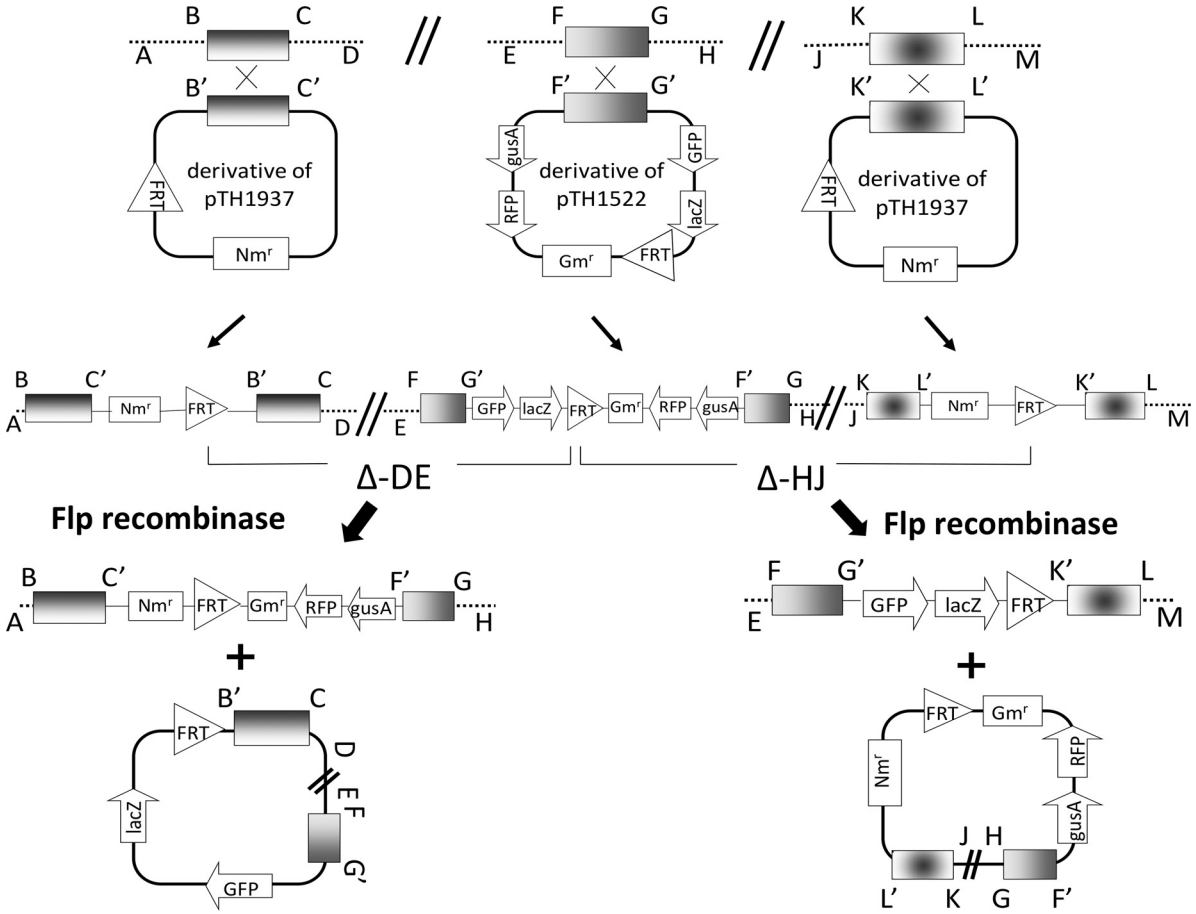

FIG 1 Schematic showing the strategy employed to generate FRT-directed deletions. Two different deletion phenotypes/genotypes result when pTH1937 integrates on either side of a single pTH1522 integrant in the genome. BC, FG, and KL are random DNA sequences that were cloned into targeting vectors. Gm^r, gentamicin resistance; Nm^r, neomycin resistance; FRT, *flp* recombinase target site; reporter genes, *gusA* and *lacZ*; GFP, green fluorescent protein; RFP, red fluorescent protein; Δ-DE, deleted region 1; Δ-HJ, deleted region 2.

Transcription analysis. Makarova et al. (1) identified 211 putative toxin or antitoxin genes in the *S. meliloti* 1021 genome. Forty-two of these genes occur within 21 contiguous gene pairs. Expression of putative toxin-antitoxin genes was examined using RNA-seq data. Briefly, RNA was prepared from *S. meliloti* P110 grown in morpholinepropanesulfonic acid (MOPS) minimal medium containing 20 μM (MOPS-P0) or 2 mM (MOPS-P2) inorganic phosphate, respectively. A directional cDNA library was prepared, and Illumina sequence reads of 34 nucleotides were obtained from it by Fasteris SA (Geneva, Switzerland). Sequence reads were aligned with the *S. meliloti* 1021 genome, and data were deposited in the GEO public functional genomics data repository under accession number GSE43558. In addition, we obtained public RNA-seq data for *S. meliloti* strain 2011 from GEO sequence accession no. GSE44083 as described by Sallet et al. (41). These data were combined, and a summary of the RNA expression of the 211 toxin-antitoxin genes that includes the *S. meliloti* gene names, the TA protein class, GI numbers, and location of each in the *S. meliloti* genome is given in Table S3 in the supplemental material. The data counts are expressed as the number of times that the 5′ end of an RNA-seq read mapped to a nucleotide within the gene regions.

Nucleotide sequence accession number. The 2,638-nucleotide sequence for pTH1937 has been deposited in GenBank under the accession number KF188463.

Microarray data accession number. Data for *S. meliloti* RmP110 were deposited in the GEO public functional genomics data repository under accession number GSE43558.

RESULTS

FRT-directed deletion strategy using targeting vectors pTH1522 and pTH1937. To delete DNA regions via Flp/FRT-directed recombination, FRT sites were inserted in direct orientation on each side of the genome region to be excised (schematic in Fig. 1). One FRT site was from a reporter fusion library of 6,000 strains in which the Gm^r suicide plasmid pTH1522, carrying a single FRT site, is integrated via single crossover recombination at known locations throughout the *S. meliloti* genome (35). The second FRT site was from the Nm^r suicide plasmid pTH1937, which carries an FRT site and a pSC101 *oriV* (see Materials and Methods). Plasmids pTH1937 and pTH1522 share insufficient homology to direct recombination, and in control experiments, no Nm^r transconjugants ($<10^{-8}$/recipient) were detected when pTH1937 was transferred into an *S. meliloti* strain carrying an integrated pTH1522. To direct pTH1937 to a particular location in the *S. meliloti* genome, 0.5 to 1.5 kb from the target region was cloned into pTH1937 and the resulting pTH1937 derivative was transferred into the target region of the appropriate *S. meliloti* ΦpTH1522 integrant strain (Fig. 1).

To catalyze recombination between the FRT sites, the tetracycline-resistant (Tc^r) Flp recombinase plasmid pTH1944 was

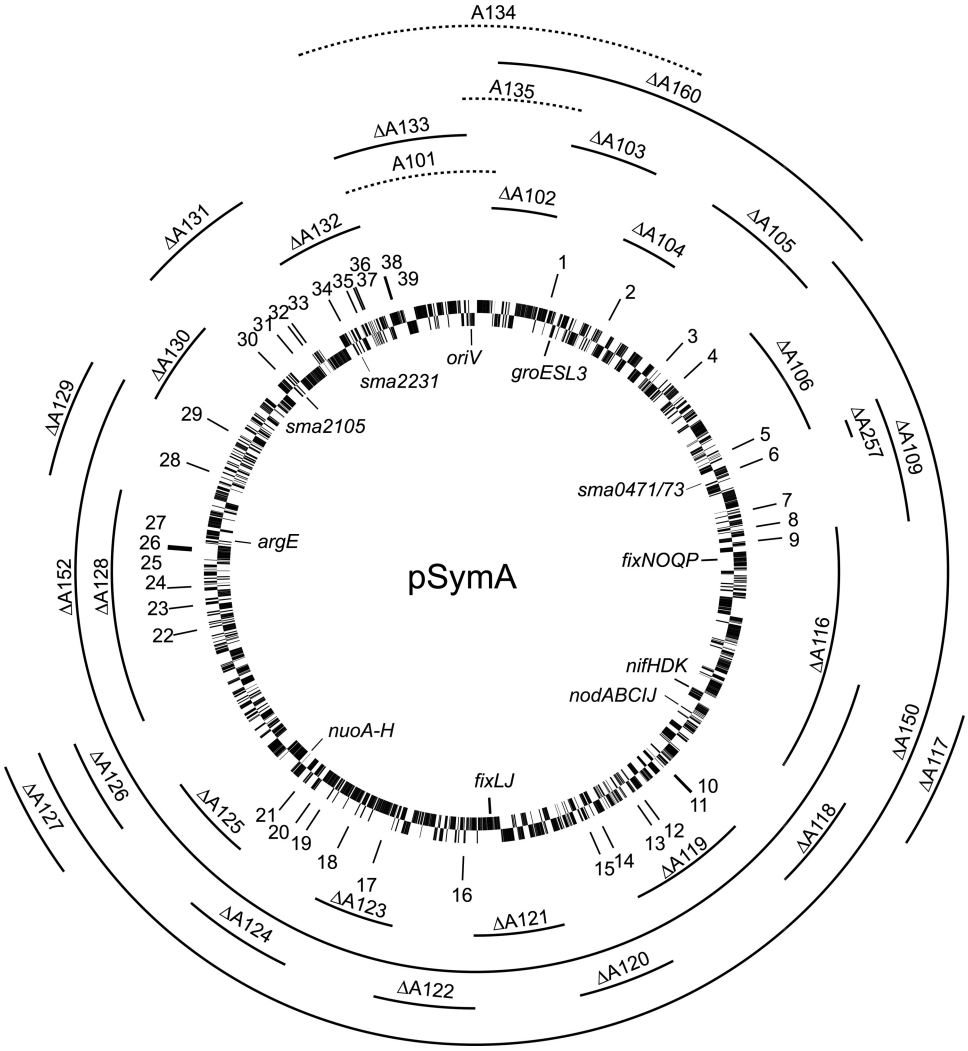

FIG 2 Circular map of the pSymA megaplasmid of *S. meliloti*, showing FRT-flanked regions generated in this study. Solid-line regions, Flp transconjugants recovered and deletions (Δ) confirmed. Dotted-line regions, Flp transconjugants not recovered. Predicted TA encoded proteins on the pSymA megaplasmid: 1, Sma5001; 2, Sma0191/Sma0193; 3, Sma0285/Sma0286; 4, Sma0319; 5, Sma0453; 6, Sma0471/Sma0473; 7, Sma0545/Sma0548; 8, Sma0572; 9, Sma0592/Sma0594; 10, Sma0917; 11, Sma5006/Sma5007; 12, Sma0967; 13, Sma0981; 14, Sma1056; 15, Sma1076; 16, Sma1253; 17, Sma5008; 18, Sma1413; 19, Sma1455/Sma1456; 20, Sma1476; 21, Sma1497; 22, Sma1725; 23, Sma1749; 24, Sma1770; 25, Sma1822; 26, Sma1823; 27, Sma1825; 28, Sma1924; 29, Sma1990; 30, Sma2105; 31, Sma2133; 32, Sma2151; 33, Sma2163; 34, Sma2231; 35, Sma2253/Sma2255; 36, Sma2273/Sma2275; 37, Sma2279/Sma2281; 38, Sma2315; 39, Sma2319.

transferred into the *S. meliloti* ΦpTH1522ΦpTH1937 double integrant strains (10^{-4}/recipient). Depending on whether the integrated pTH1522 lay upstream or downstream from the integrated pTH1937, the resulting deletion strain was either Sm^r Gm^r Nm^r Tc^r, with the pTH1522-carried *lacZ* gene lost, or Sm^r Gm^s Nm^s Tc^r, with the pTH1522-carried *lacZ* gene retained (Fig. 1, Δ-DE and Δ-HJ, respectively).

We note that even when the deleted region carried essential genes, Tc^r Flp recombinase transconjugants were still recovered, albeit at a reduced frequency. These transconjugants arose as a result of loss of one of the FRT sites by spontaneous RecA-directed resolution of the ΦpTH1522 cointegrate or of the ΦpTH1937 cointegrate. Hence, Tc^r Flp recombinase plasmid transconjugants were screened for their Gm^r, Nm^r, and LacZ phenotypes (Fig. 1), and as described below, purified putative deletion strains were then analyzed by PCR.

Construction and confirmation of the pSymA and pSymB megaplasmid deletions. Eighty-nine FRT-flanked regions of pSymA or pSymB were assigned ascending numbers from A100 and B100, respectively. The precise boundaries of the FRT sites are given in Table S1 in the supplemental material, and schematics showing a subset of the regions from pSymA and pSymB are shown in Fig. 2 and 3, respectively. Following transfer of the Flp recombinase to these strains, PCR was used to amplify and detect gene regions located inside and outside the FRT deletion endpoints and thus confirm, or not, that the FRT-flanked regions were deleted. For example, Fig. 4 shows a schematic and the PCR products obtained for the B123 region of pSymB before and after transfer of the Flp plasmid to the B123 strain. PCR products internal to the B123 region are clearly present in the B123 strain prior to transfer of the Flp plasmid (Fig. 4, lanes 6 and 7), while these fragments are absent in the B123 strain carrying the Flp

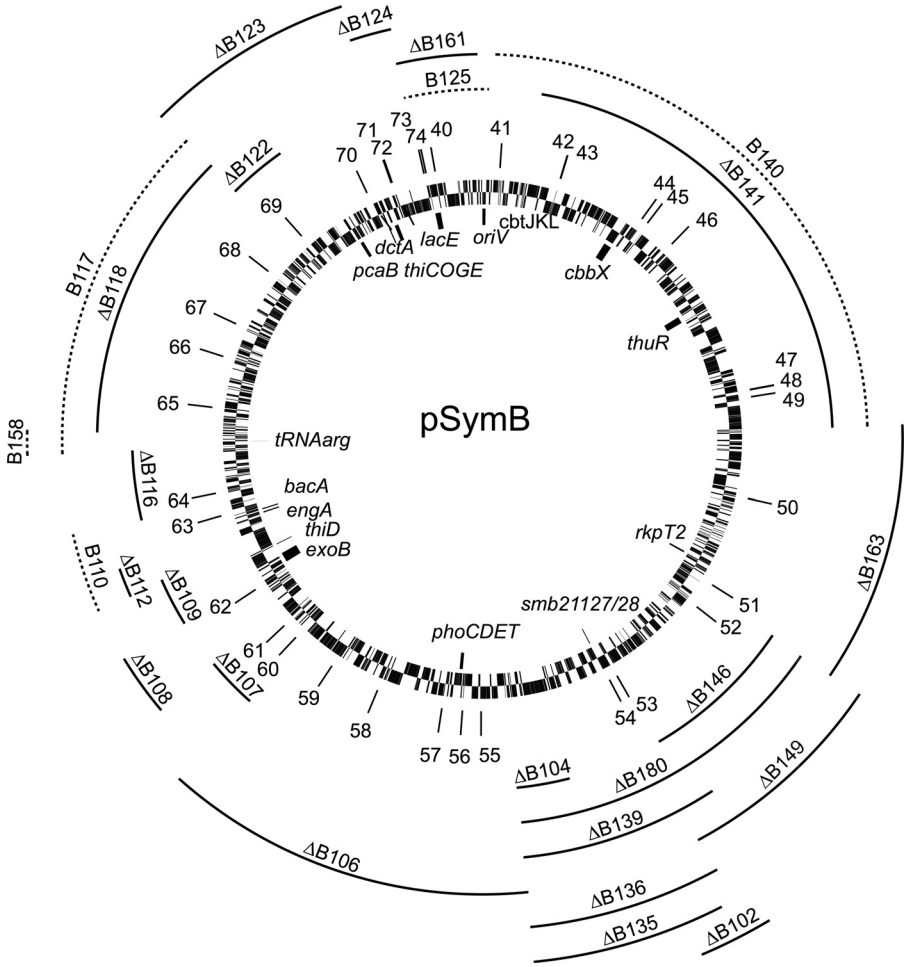

FIG 3 Circular map of the pSymB megaplasmid of *S. meliloti*, showing FRT-flanked regions, generated in this study. Solid-line regions, Flp transconjugants recovered and deletions (Δ) confirmed. Dotted-line regions, Flp transconjugants not recovered. Predicted TA encoded proteins on the pSymB megaplasmid: 40, Smb20005; 41, Smb20062/Smb20063; 42, Smb22004; 43, Smb20121; 44, Smb20215; 45, Smb20222; 46, Smb20256; 47, Smb20411; 48, Smb20412/Smb20413; 49, Smb20420; 50, Smb22021; 51, Smb20835; 52, Smb21035; 53, Smb21117; 54, Smb21127/Smb21128; 55, Smb21153; 56, Smb21169; 57, Smb21187; 58, Smb21336; 59, Smb21670; 60, Smb21559; 61, Smb21576; 62, Smb20935; 63, Smb21007/Smb21008; 64, Smb20859; 65, Smb21419; 66, Smb21475/Smb21476; 67, Smb21509/Smb21510/Smb21511; 68, Smb20695/Smb20696; 69, Smb20754; 70, Smb20607/Smb20608; 71, Smb20626; 72, Smb20627/Smb20628/Smb20629; 73, Smb21649; 74, Smb21651.

plasmid (lanes 2 and 3, loci C and D). A region from the chromosome was amplified as a control in all reactions (region Y in Fig. 4). These data confirmed the gross structure of the ΔB123 deletion, and all of the deletion strains were similarly confirmed by PCR (see Table S1). When the deletion was verified with respect to the presence/absence of antibiotic resistance and PCR markers, the deletion was designated with a Δ (e.g., ΔB118).

Megaplasmid pSymA and pSymB deletion analyses. Individual deletion strains (ΔA102 to ΔA133) which together removed all of pSymA except the 10-kb *oriV* region were recovered (e.g., ΔA101). The isolation of the ΔA102 to ΔA133 strains suggested that pSymA does not carry any essential genes, as expected considering that pSymA has previously been cured from *S. meliloti* (22). We therefore expected that the transfer of Flp recombinase to pSymA carrying the FRT-flanked A101, A134, or A135 region would result in the recovery of strains that retained the A101, A134, or A135 region and lost the remainder of pSymA; however, no such strains were recovered. These results, together with findings that several of the deletions that were generated via Flp recombinase could not be transferred (transduced) into the wild-type RmP110 (see below), led us to identify three pSymA regions that carried active toxin-antitoxin systems.

The pSymB megaplasmid is 1,683,333 bp in size, and its DNA sequence is numbered clockwise, with nucleotide position 1 annotated as the A of the ATG start codon of the *lacE* gene (4). Fifty-six double integrant strains that carried FRT sites in direct orientation in the pSymB megaplasmid were made (Fig. 3). As outlined previously, deletions that removed the B110 and B117 regions were recovered only when the essential *engA* (B110) and Arg-tRNA (B117) genes were present in *trans* on a replicating plasmid or integrated into the chromosome (29). Deletion mutants that removed the *smb20056* to *-20059* gene cluster (e.g., ΔB140) were recovered only when the pTH1944-*flp* transconjugants were selected on LB medium supplemented with $CoCl_2$ (2 ng/ml) since the *smb20056-smb20057-smb20058* genes encode an ABC-type cobalt transport system (*cbtJKL*) required for growth of RmP110 in LB (42). Furthermore, the inability to efficiently transfer the megaplasmid deletions into wild-type recipient strains by

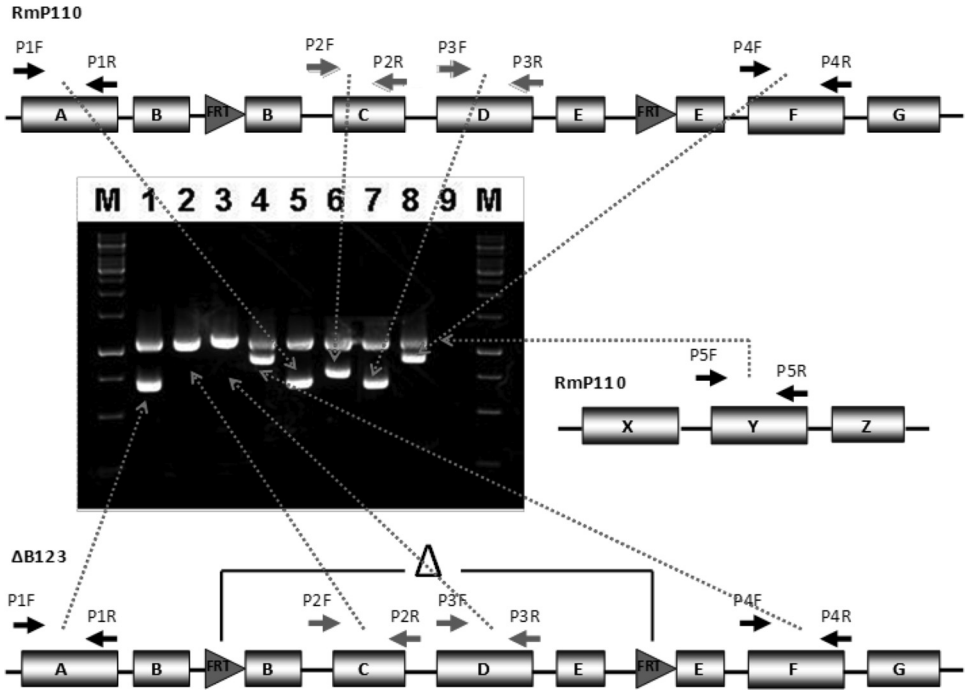

FIG 4 Schematic outline of the PCR amplification method used to examine deletion structure. Primer pairs P1 and P4 amplified DNA fragments on either side of the targeted FRT-flanked region. Primer pairs P2 and P3 amplified DNA fragments inside the FRT-targeted region. Amplified products were separated and visualized by agarose gel electrophoresis. Lanes 5 to 8, DNA from wild-type strain RmP110; lanes 1 to 4, DNA from the ΔB123 strain; lane 9, no template DNA control; lanes M, molecular weight marker (GeneRuler 1-kb DNA ladder; Fermentas). The upper band in lanes 1 to 8 is a DNA fragment from the chromosomal region of wild-type strain RmP110 amplified with primer pair P5.

transduction led to the identification of an active pSymB toxin-antitoxin system (see below).

However, even when *engA* and the Arg-tRNA were present in *trans*, and excess cobalt (2 ng/ml) was included in the medium, deletions that remove the pSymB *oriV* region (e.g., ΔB125) were not recovered. Thus, for both pSymA and pSymB, deletions that removed the megaplasmid replication origins were not recovered.

Identification of toxin-antitoxin systems. In performing a genetic analysis of the pSymA and pSymB deletion strains, we observed that the Gm^r Nm^r-marked deletions ΔA131 (nt 1173730 to 1231998), ΔA132 (nt 1232916 to 1283082), ΔA257 (nt 255655 to 262769), and ΔB139 (nt 740722 to 869642) could not be recombined via transduction into the wild-type recipient RmP110. In control experiments, the individual FRT insertions used in the construction of the ΔA131, ΔA132, ΔA257, and ΔB139 deletions were readily recombined via transduction into wild-type strain RmP110 (frequency, ~10^{-7}/recipient). These data suggested that loss of a gene(s) within the A131, A132, A257, and B139 regions prevented recovery of ΔA131, ΔA132, ΔA257, and ΔB139 recombinants, respectively, and below, we show that the responsible genes encoded toxin-antitoxin systems. We note that while the ΔA131, ΔA132, ΔA257, and ΔB139 deletion strains were originally recovered via Flp recombinase-directed deletion, in repeat experiments the recovery of these deletions was observed to occur at a very low frequency.

Bioinformatic analysis of the *S. meliloti* 1021 genome identified 211 genes predicted to encode type II toxin or antitoxin proteins (1, 32). We extracted these genes from supplemental data reported by Makarova et al. (1), and a summary showing the distribution of these TA genes among the three *S. meliloti* replicons is shown in Table 1. The locations of the TA-associated genes on the pSymA and pSymB megaplasmids are shown in Fig. 2 and 3, and detailed coordinates for each gene are given in Table S3 in the supplemental material.

Toxin-antitoxin gene s*ma2105* on the pSymA megaplasmid. The inability to transduce ΔA131 (nt 1173730 to 1231998) into RmP110 prompted an examination of the genes present in the 60-kb A131 region (Fig. 5B). Three genes, *sma2105* (1,221 bp), *sma2133* (792 bp), and *sma2151* (324 bp), are predicted members of the toxin-antitoxin families Fic, Xre, and Xre, respectively (1, 19). These loci, together with the upstream promoter regions, were cloned into the Sp^r pTH1931 vector to generate the plasmids pTH2646, pTH2647, and pTH2622, respectively. When RmP110 carried the *sma2105* gene (pTH2646) in *trans*, transduction of the Gm^r Nm^r-marked ΔA131 deletion into wild-type RmP110 occurred (frequency, ~10^{-7}/recipient), while no transductants were obtained when *sma2133* (pTH2647) or *sma2151* (pTH2622) was present in *trans* (Table 2 and data not shown). The pTH1522 integrant (FL4094) used in the construction of ΔA131 was readily transduced into all these strains. The role of the region upstream of the *sma2105* gene in transduction of the Gm^r Nm^r-marked ΔA131 deletion was also examined. The region upstream of *sma2105* (nt 1187240 to 1187703) was cloned in the pTH1931 vector as a 463-bp fragment to generate the plasmid pTH2790 (Fig. 5B). Transduction of the Gm^r Nm^r-marked ΔA131 deletion into wild-type RmP110 occurred (frequency, ~10^{-7}/recipient) when RmP110 carried the upstream region of *sma2105*. The region upstream of *sma2105* therefore appears to carry an antitoxin gene, and how this controls toxin activity requires further investigation.

TABLE 1 Predicted toxin and antitoxin protein classes in the genome of *S. meliloti* 1021[a]

Type[b]	No. found in:			
	pSymA	pSymB	Chromosome	Genome
AbrB			7	7
ArsR	2	4	11	17
COG2442	1			1
COG2856		1	1	2
COG2929			1	1
COG3832	3	6	14	23
COG5642	2	2		4
COG5654	2	2		4
Fic	2[b]		1	3
GNAT		2	11	13
HEPN	1	1	1	3
HicA			1	1
HicB			3	3
HipA	1		1	2
MazF		2		2
MazFn	1			1
MNT	2	1		3
PHD	1		3	4
PIN	8	4	12	24
RelE	5	3	8	16
RHH	5	6	12	23
Xre	14	13	27	54
Total	50	47	114	211

[a] Data were extracted from TA genes predicted by Makarova et al. (1).
[b] Sma2105 has two Fic domains, Smb20754 and Smc00769 each have COG2856 and Xre domains, and Smb20835 has HEPN and MNT domains. The open reading frame upstream of *sma2231* is not included in the table.

Toxin-antitoxin system *orf2230/sma2231* on the pSymA megaplasmid. The 53-kb ΔA132 deletion (nt 1232916 to 1283082) could not be transduced into the wild-type RmP110, and three toxin-antitoxin loci lay within this region: *sma2231* (384 bp), *sma2253/sma2255* (378/339 bp, respectively), and *sma2273/sma2275* (351/276 bp, respectively) (1). While *sma2231* initially appeared to be an isolated toxin gene, analysis of the 754-nt region upstream of *sma2231* allowed us to identify a putative open reading frame (Fig. 5C). This open reading frame, designated *orf2230*, encoded a 66-amino-acid protein whose TTG stop codon overlaps the *sma2231* GTG start codon by a single nucleotide. We sought to clone the *orf2230/sma2231*, *sma2253/sma2255*, and *sma2275/sma2273* genes with their corresponding promoter regions into the Sp^r pTH1931 vector. The clone of *sma2253/sma2255* together with a possible 66-amino-acid antitoxin upstream of *sma2253* was not recovered in *E. coli*; however, pTH1931 clones carrying only *sma2253* and the putative upstream antitoxin were recovered. *orf2230/sma2231* and *sma2275/sma2273*, together with their promoter regions, were cloned into pTH1931 to form pTH2623 and pTH2625, respectively. Transduction of ΔA132 (Gm^r Nm^r) into RmP110 carrying these plasmids occurred only when RmP110 carried the *orf2230/sma2231* genes in *trans* (frequency, 1×10^{-7}/recipient) (Table 2). No recombinants were obtained when ΔA132 was transduced into RmP110 carrying *sma2253* or *sma2275/sma2273* in *trans*.

Toxin-antitoxin system *sma0471/sma0473* on the pSymA megaplasmid. The ability to transduce ΔA152 (nt 402136 to 1122176) and not ΔA150 (nt 186200 to 930000) into RmP110 suggested that a gene(s) within the nt 193611 to 400267 region was responsible for this phenotype. Further deletion analysis of this large region (data not shown) allowed us to localize the region that was recalcitrant to deletion to a 9-kb region (nt 255655 to 264696) carrying nine annotated genes. Of these genes, *sma0471/sma0473* were identified as responsible for the failure to transduce ΔA257 (nt 255655 to 262769), as the presence of these genes in *trans* on a replicating plasmid (pTH2563) (Fig. 5A) in the RmP110 recipient allowed transduction of the ΔA257 deletion (10^{-7}/recipient) (Table 2).

Toxin-antitoxin system *smb21127/smb21128* on the pSymB megaplasmid. Very few colonies were recovered upon transduction of the ΔB139 (nt 740722 to 869642) deletion into RmP110 (10^{-9}/recipient). Examination of this region revealed a putative TA locus, *smb21127/smb21128*, and, at a separate location, a single putative antitoxin gene, *smb21117*. As the *smb21127/smb21128* locus is the only one predicted to encode a toxin, this gene pair was cloned into pTH1931, producing pTH2830 (Fig. 5D). The presence of these genes in *trans*, or just the putative antitoxin *smb21127*, allowed the recovery of ΔB139 transductants at a frequency of 10^{-7}/recipient (Table 2 and data not shown). Furthermore, disruption of the putative toxin gene *smb21128* allowed subsequent transduction of ΔB180 (nt 635940 to 869642) at a frequency of 10^{-7}/recipient (data not shown). These data confirmed that *smb21127/smb21128* encode an active toxin-antitoxin system.

Effect of TA systems on the growth of *S. meliloti*. The effect of the toxin-antitoxin-like loci on the growth and cell viability of *S. meliloti* was monitored by deleting the megaplasmid regions in strains with or without the TA loci in *trans*. The in *trans* copy of the appropriate TA loci was present as an insert on the replicating pTH1931 (Sp^r) plasmid, and the FRT-flanked regions were then deleted via the IPTG-dependent induction of *flp* from pTH1944 (Tc^r). Additional control strains included a strain in which FRT sites flanked the pSymA *oriV* (A101), a strain in which FRT sites flank a pSymA region that could be deleted without any apparent effect (A128), and a strain in which the essential Arg-tRNA gene of pSymB is flanked by FRT sites (B158). All these strains were grown overnight in LBmc medium and diluted to an OD_{600} of 0.03 to 0.04, and half of the resulting cultures were grown with 0.5 mM IPTG and half without IPTG. The optical density (OD_{600}) and cell viability of the resulting cultures were monitored over a 24-h period (Fig. 6).

In all experiments, deletion of the tRNA^{Arg} gene region (B158) and the pSymA *oriV* (A101) region resulted in decreased growth and 100-fold and 1,000-fold drops in cell viability, respectively (Fig. 6). Deletion of the *sma2105* and *orf2230/sma2231* TA loci also appeared to have a bactericidal effect, as a >10-fold drop in cell viability was observed, while the deletion of *sma0471/sma0473* and *smb21127/smb21128* loci was bacteriostatic. Importantly, the presence of the appropriate TA locus in *trans* appeared to completely rescue the observed growth phenotypes, while none of the TA loci individually rescued the decrease in cell density and viability that resulted from the deletion of the pSymA *oriV* (ΔA101).

DISCUSSION

We have generated deletion strains that collectively removed most of the 1.35-Mb pSymA and 1.68-Mb pSymB megaplasmids of *S. meliloti*. About 100 toxin (T) or antitoxin (A) genes are located on the pSymA and pSymB replicons (1, 32) (Table 1), and if the

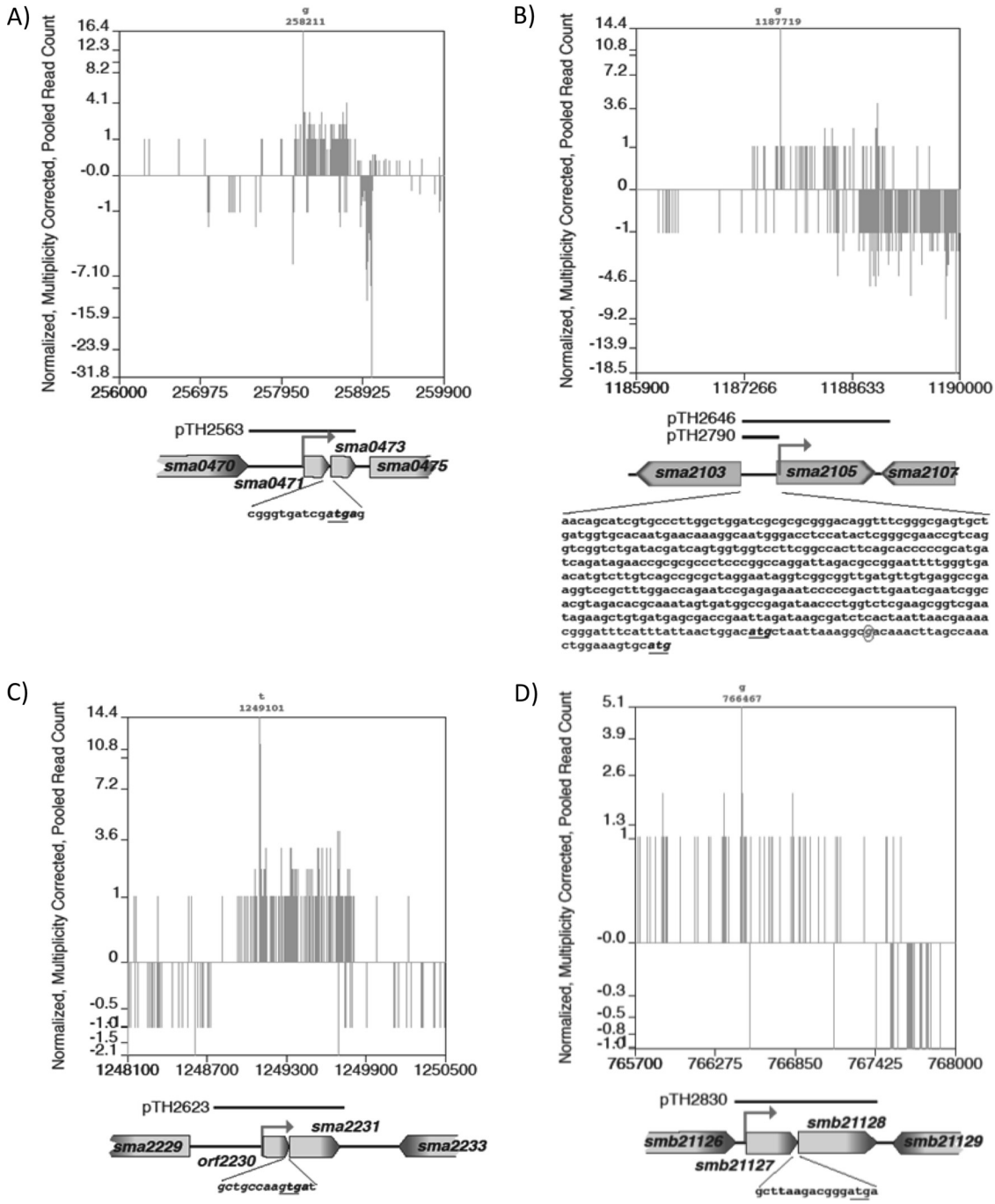

FIG 5 Schematic of the four toxin-antitoxin loci showing the 5′ RNA-seq read counts across the gene regions and the DNA fragments employed for complementation analyses: *sma0471*/*sma0473* (A), *sma2105* (B), *orf2230*/*sma2231* (C), and *smb21127*/*smb21128* (D). For panels A, C, and D, the start/stop codons are indicated, and for panel B, the sequence upstream of *sma2105*, including the two start codons and the predicted transcription start site, is indicated. The transcription start sites for the transcripts are shown as solid arrows, and the nucleotide position of the transcription start site is given above each plot. The plots show the frequency and direction (+ or −) of where the 5′ nucleotide of each 34-nt mRNA (cDNA) sequence read corresponded to the nucleotide position of the indicated gene region. These data were taken from the perfectly matched sequence reads from the P0 experiment and were normalized against the P2 reads so that the total read count matched.

production of the toxin and that of the antitoxin are simultaneously disrupted, the residual antitoxin quickly degrades, liberating the toxin to exert its effect. Thus, when a TA locus is lost from a cell, potentially through a genome deletion event, the toxin is released and is generally expected to promote cell death or stasis in a large majority of the population. We identified only four TA loci whose deletion dramatically affected cell growth (*sma0471*/*sma0473*, *sma2105*, *orf2230*/*sma2231*, and *smb21127*/*smb21128*), and we discuss these loci below.

The 102- and 97-amino-acid proteins encoded by *sma0471* and

TABLE 2 Frequency of recombination of *S. meliloti* megaplasmid deletions into wild-type strains carrying the empty plasmid vector pTH1931 or pTH1931 containing TA genes[a]

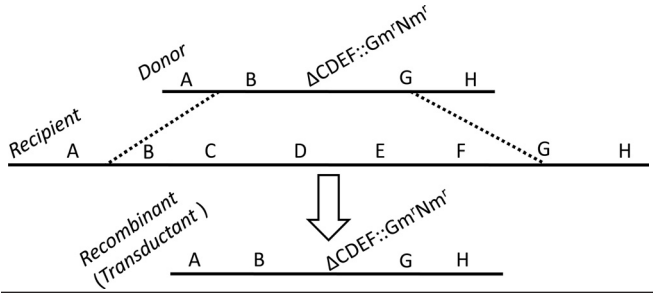

Phage donor → recipient strain	Transductant colonies per plate (frequency/recipient)[b]
ΦΔA257 → WT(pTH1931-*sma0471/73*)	120 (1×10^{-7})
ΦΔA257 → WT(pTH1931)	2 (2×10^{-9})
ΦΔA131 → WT(pTH1931-*sma2105*)	99 (4×10^{-7})
ΦΔA131 → WT(pTH1931-upstream region of *sma2105*)	20 (1×10^{-7})
ΦΔA131 → WT(pTH1931)	0 ($<10^{-9}$)
ΦΔA132 → WT(pTH1931-*sma2230/31*)	30 (1×10^{-7})
ΦΔA132 → WT(pTH1931)	0 ($<10^{-9}$)
ΦΔB139 → WT(pTH1931-*smb21127/28*)	107 (4×10^{-7})
ΦΔB139 → WT(pTH1931)	5 (1×10^{-8})

[a] The diagram above the table illustrates the two homologous recombination events (dashed lines) that occur in transduction of deletion ΔCDET::Gm^r Nm^r from a donor strain into a wild-type recipient. The structure of the resulting Gm^r Nm^r transductant (recombinant) is shown. Similarly, the Gm^r Nm^r-marked ΔA257, ΔA131, ΔA132, and ΔB139 deletions (Fig. 2 and 3) were transduced using phage ΦM12 into RmP110 wild-type (WT) recipient strains carrying the empty Sp^r plasmid vector pTH1931 or pTH1931 carrying the TA gene regions as indicated.

[b] Numbers of transductant colonies per plate as well as transductional frequency per recipient for each transduction are indicated. Results are representative of three independent experiments.

sma0473 are closely related to the RelB antitoxin and RelE toxin proteins, respectively (43). The RelBE family is distributed in a wide variety of bacteria and archaea (1, 43). RelE toxicity results from cleavage of mRNA at the ribosomal A site as it is being translated (44). In a recent report, six RelE-like proteins from different phyla, including the 98-amino-acid SMc00822 protein from the chromosome of *S. meliloti*, were shown to inhibit translation by cleaving ribosome-associated transcripts (45). In general, cells exposed to the RelE toxin show a drastic growth arrest (39, 46, 47). In accordance, the deletion of *sma0471/sma0473* in *S. meliloti* resulted in a bacteriostatic phenotype [Fig. 6, A257(pTH1931) versus A257(pTH1931) (+IPTG)], presumably due to the decay of the Sma0471 antitoxin and the resulting release of active Sma0473 toxin.

The second locus whose deletion was toxic to *S. meliloti* was *sma2105*. The domain organization of Sma2105 suggests that it may be a Doc (death on curing)-type toxin, the toxic component of the *phd/doc* TA family (48). Sma2105 has a Fic-N domain (residues 41 to 125) and a FIC domain (130 to 235) common to the Doc proteins, as well as the conserved central motif of 9 residues, HXFX[D/E]GNGR (43). The *phd/doc* operon encodes a TA module aiding the maintenance of the plasmid-prophage P1 in *E. coli* (5), and free Doc protein inhibits translation elongation via association with the 30S ribosomal subunit, which subsequently leads to growth arrest in *E. coli* (49). In *S. meliloti*, the deletion of the *sma2105* locus resulted in a bactericidal effect [Fig. 6, A131(pTH1931) versus A131(pTH1931) (+IPTG)].

Examination of both RNA-seq data and alignments of Sma2105 and its orthologs indicated that the actual ATG start codon for Sma2105 is 14 amino acids further into the gene than originally annotated in Rm1021, and this is corrected in the Rm2011 annotation (18, 41). Interestingly, *sma2105* is annotated as being carried by a monocistronic mRNA, without a cognate antitoxin. Moreover, there is a large 500-nt region upstream of *sma2105* with no annotated gene, and plasmid clones carrying only this region allowed the deletion of *sma2105* (Table 2). There is no evidence of a protein-coding region or small RNA present in this upstream region; therefore, it seems unlikely that this upstream region encodes an antitoxin to the Sma2105 toxin, although this cannot be fully ruled out. An intriguing possibility is that Sma2105 represents a novel toxin-antitoxin family. Unlike other Doc proteins, Sma2105 appears to contain a MarR-like DNA-binding domain in the C-terminal domain. Perhaps, Sma2105 binds to the region upstream of *sma2105*, and this association prevents the protein from exerting its toxic effect; thus, only when the concentration of Sma2105 exceeds that of its DNA-binding site would it show a bactericidal effect. Further studies are required to resolve the organization of this locus and the nature of this predicted interaction.

The third toxic TA system encodes the Orf2230 antitoxin and the Sma2231 toxin proteins. Sma2231 is a member of the ~130-amino-acid PIN-domain protein family, whose proteins are often the toxic components of *vapBC* TA systems (50). VapC toxins containing a PIN domain block protein translation via mRNA cleavage (51). In *vapBC* systems, the VapB protein is generally coexpressed with VapC and it inhibits VapC RNase activity. Makarova et al. (1) reported that 21 of 24 PIN-domain proteins in *S. meliloti* are present as *vapBC* TA systems (12 on chromosome, 8 on pSymA, and 4 on pSymB). While *sma2231* initially appeared to be an isolated *vapC*-like gene, there is a 754-nt region upstream of *sma2231*. Analysis of this region allowed us to identify a putative open reading frame, designated *orf2230*, upstream of *sma2231* encoding a 66-amino-acid protein. As is common in *vapBC* operons, the TTG stop codon of *orf2231* overlaps the *sma2231* GTG start codon by a single nucleotide (50). The Orf2230 protein contains a domain of unknown function (DUF2191), which is also present in multiple VapB homologs in *Mycobacterium tuberculosis* (51). Unlike the bacteriostatic effect observed to be associated with VapC toxins from *Mycobacterium smegmatis* and *M. tuberculosis*, our analysis showed that deleting *orf2230/sma2231* (ΔA132) had a bactericidal effect (52, 53).

The only active TA system detected on pSymB was the *smb21127/smb21128* locus. The gene for the predicted toxin, Smb21128, encodes a 184-amino-acid hypothetical protein from the COG5654 and pfam08808 families. These proteins share a RES domain, so named because they share three highly conserved polar amino acids, arginine (R), glutamate (E), and serine (S), which possibly form an active site with nuclease activity (54). *smb21127* encodes a 123-amino-acid hypothetical antitoxin from the COG5642 and pfam09722 families, and these proteins carry an Xre DNA-binding domain that is commonly found in phage repressor proteins (55). Based on a bioinformatics analysis, Makarova et al. (1) suggested that COG5654-Xre (COG5642) gene pairs could function as TA systems. However, we are unaware of any experimental data to confirm this hypothesis. Our data

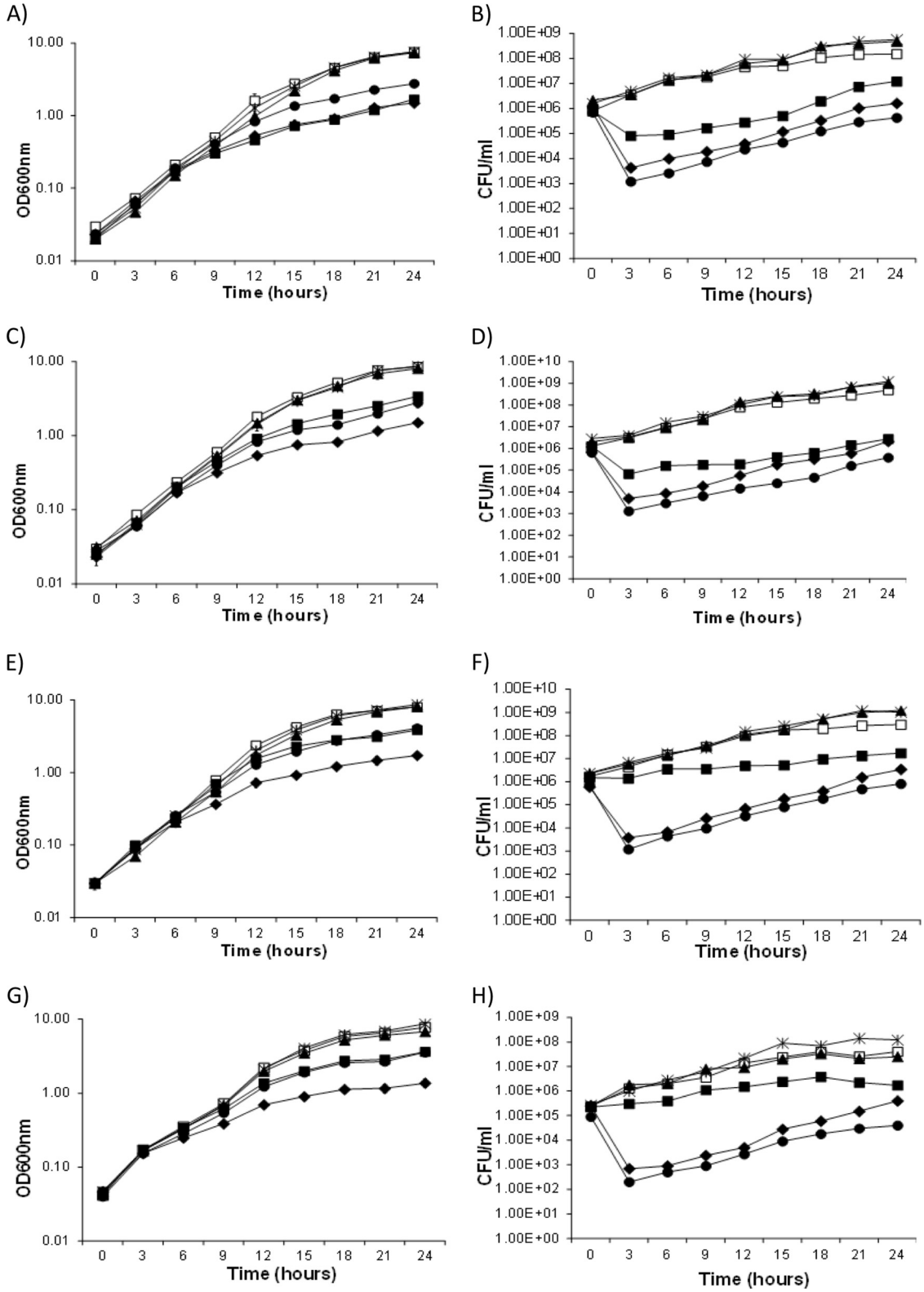

FIG 6 Effects on the growth of *Sinorhizobium meliloti* resulting from the Flp-catalyzed deletion of four separate TA loci. Cells were grown in LBmc, and Flp recombinase was induced by addition of IPTG at time zero. Growth was monitored by measuring the optical density at 600 nm, and viable cell count was measured as CFU. The TA loci were deleted in strains carrying the cognate TA gene region in *trans* on the plasmid pTH1931 and in strains carrying empty pTH1931. In addition, all experiments included the three strains A101, A128, and B158. In *S. meliloti* strain A101, the *oriV* of pSymA is flanked by FRT sites. In strain A128, FRT sites flank a nonessential region of pSymA that carries six TA-associated genes. Strain B158 carries FRT sites flanking the essential $tRNA^{Arg}$ gene

showed that the deletion of *smb21127/smb21128* had a bacteriostatic effect on *S. meliloti* (Fig. 6), and in further work, we found that providing the antitoxin *smb21127* on pTH1931 in *trans* was sufficient to allow deletion of the *smb21127/smb21128* region. These data suggest that the *smb21127/smb21128* operon functions as an active toxin-antitoxin system and provide the first experimental evidence that COG5654-COG5643 gene pairs can function as TA systems.

Of the ~100 TA-associated genes that have been identified on the pSymA and pSymB megaplasmids (Table 1), this deletion analysis identified only four "active" systems. In comparison, 30 of 88 putative TA systems of *M. tuberculosis* were shown to be functional (51). We were curious as to why so few of the predicted TA systems showed a severe growth phenotype following their deletion. One possibility is that many of the predicted TA loci do not function as TA systems. These loci were predicted to function as TA systems based on a bioinformatics approach; thus, it is possible that some were misclassified (1). Alternatively, some of these loci may contain TA system pseudogenes whose activity has decayed. For example, studies of the ccd_{O157} toxin in *E. coli* indicate that there are several alleles of this toxin, 30% of which are not toxic (56).

While it is likely that some of the megaplasmid systems are indeed not active, we suspect that many are functional. In TA systems, the toxin-antitoxin protein complex generally negatively regulates its own expression; it is only following protease (Lon or Clp)-mediated degradation of the antitoxin that the locus is expressed at high levels (2, 6). Thus, we hypothesized that many of the TA systems may be expressed at low levels, and if functional, there may be insufficient toxin present to kill the cell following deletion of the locus. We therefore investigated the expression of the TA genes of *S. meliloti* by analyzing strand-specific RNA-seq data obtained with RNA from wild-type (RmP110) cells grown with excess phosphate and under phosphate-limiting stress conditions. We also examined RNA-seq data from a recently published *S. meliloti* 2011 (which is derived from the parent strain SU47, as is RmP110) data set obtained from exponentially growing and stationary-phase cells, as well as from bacteroids isolated from 10-day-old nodules from *Medicago truncatula* (41). Interestingly, while *sma0471/sma0473* and *smb21127/smb21128* were highly expressed relative to the other TA genes on pSymA and pSymB, the *sma2105* and *sma2231* genes were expressed at quite low levels. Moreover, the patterns of expression of the megaplasmid genes and those on the chromosome were similar (Fig. 7A and B; see also Table S3 in the supplemental material). Hence, the toxicity of the "active" TA genes does not appear to be a direct reflection of their level of transcription prior to deletion.

The ability to identify active toxin-antitoxin modules through a deletion analysis may also be affected by cross-interactions between the various systems. While some studies in *Caulobacter crescentus* and *M. tuberculosis* suggest that TA pairs belonging to the same family are independent functional units, other studies with *M. tuberculosis* and *E. coli* suggest that TA systems interact with each other both transcriptionally and via modulation of toxin activities (51, 57–60). Of 211 TA-associated genes in *S. meliloti*, representatives include 54 Xre proteins (27 chromosomal), 24 PIN proteins (12 chromosomal), 22 COG3832 orthologs (14 chromosomal), and 16 RelE orthologs (8 chromosomal) (Table 1). Thus, many putative interactions may exist that could mask the activity of these loci when deleted individually; clearly unraveling such interactions will require further studies.

Although not always the case, various studies have shown a link between TA modules and many biological functions (7, 11). Toxin-antitoxin loci were initially identified due to their ability to stabilize plasmids through mediating postsegregation killing (12). Subsequently, chromosomal TA systems were suggested to stabilize large, nonessential chromosomal regions. The "active" TA genes in the *S. meliloti* megaplasmids may prevent the deletion of large regions from these megaplasmids and contribute to the overall stability of these replicons. While pSymA has previously been removed from *S. meliloti* in its entirety through sequential deletions (30), we were unable to remove pSymA in a single step. Experiments are under way to simultaneously provide the antitoxins for *sma0473*, *sma2105*, and *sma2231* in *trans* to determine if this will allow for all of pSymA to be simultaneously deleted. In addition to stabilization, TA systems have been suggested to function as a defense mechanism against phage infection, in adaptation to stress, and as a regulator of developmental processes, including pathogenesis, biofilm formation, and sporulation (7, 11).

Although we have not analyzed the TA systems reported here in respect to their biological role, an intriguing possibility is that they could be involved in the developmental process leading to a successful symbiosis with host legumes. Indeed, deletion of the *vapBC*-type TA module, designated *bat/bto*, from the soybean symbiont *Bradyrhizobium japonicum* resulted in a reduced symbiotic phenotype, although this may have been due to an indirect pleiotropic effect as the deletion mutant had altered cell morphol-

on pSymB. (A and B) *sma0471/sma0473*. Growth (OD_{600}) (A) and viable counts (CFU/ml) (B) of strain A257(pTH1931), strain A257(pTH1931-*sma0471/sma0473*), and the three control strains in LB medium with or without IPTG. In *S. meliloti* strain A257, FRT sites flank a 24.5-kb region that includes *sma0471/sma0473*. Symbols: open squares, A257(pTH1931); filled squares, A257(pTH1931) (+IPTG); filled triangles, A257(pTH1931-*sma0471/sma0473*) (+IPTG); filled diamonds, A101(pTH1931-*sma0471/sma0473*) (+IPTG); asterisks, A128(pTH1931-*sma0471/sma0473*) (+IPTG); filled circles, B158(pTH1931-*sma0471/sma0473*) (+IPTG). (C and D) *sma2105*. Growth (OD_{600}) (C) and viable counts (CFU/ml) (D) of strain A131(pTH1931), strain A131(pTH1931-*sma2105*), and the three control strains in LB medium with or without IPTG. In strain A131, FRT sites flank a 40-kb region that includes *sma2105*. Symbols: open squares, A131(pTH1931); filled squares, A131(pTH1931) (+IPTG); filled triangles, A131(pTH1931-*sma2105*) (+IPTG); filled diamonds, A101(pTH1931-*sma2105*) (+IPTG); asterisks, A128(pTH1931-*sma2105*) (+IPTG); filled circles, B158(pTH1931-*sma2105*) (+IPTG). (E and F) *orf2230/sma2231*. Growth (OD_{600}) (E) and viable counts (CFU/ml) (F) of strain A132(pTH1931), strain A132(pTH1931-*orf2230/sma2231*), and the three control strains in LB medium with or without IPTG. In strain A132, FRT sites flank a 40-kb region that includes *orf2230/sma2231*. Symbols: open squares, A132(pTH1931); filled squares, A132(pTH1931); filled triangles, A132(pTH1931-*orf2230/sma2231*) (+IPTG); filled diamonds, A101(pTH1931-*orf2230/sma2231*) (+IPTG); asterisks, A128(pTH1931-*orf2230/sma2231*) (+IPTG); filled circles, B158(pTH1931-*orf2230/sma2231*) (+IPTG). (G and H) *smb21127/smb21128*. Growth (OD_{600}) (G) and viable counts (CFU/ml) (H) of strain B139(pTH1931), strain B139(pTH1931-*smb21127/smb21128*), and the three control strains in LB medium with or without IPTG. In strain B139, FRT sites flank a 129-kb region that includes *smb21127/smb21128*. Symbols: open squares, B139(pTH1931); filled squares, B139(pTH1931) (+IPTG); filled triangles, B139(pTH1931-*smb21127/smb21128*) (+IPTG); filled diamonds, A101(pTH1931-*smb21127/smb21128*) (+IPTG); asterisks, A128(pTH1931-*smb21127/smb21128*) (+IPTG); filled circles, B158(pTH1931-*smb21127/smb21128*) (+IPTG).

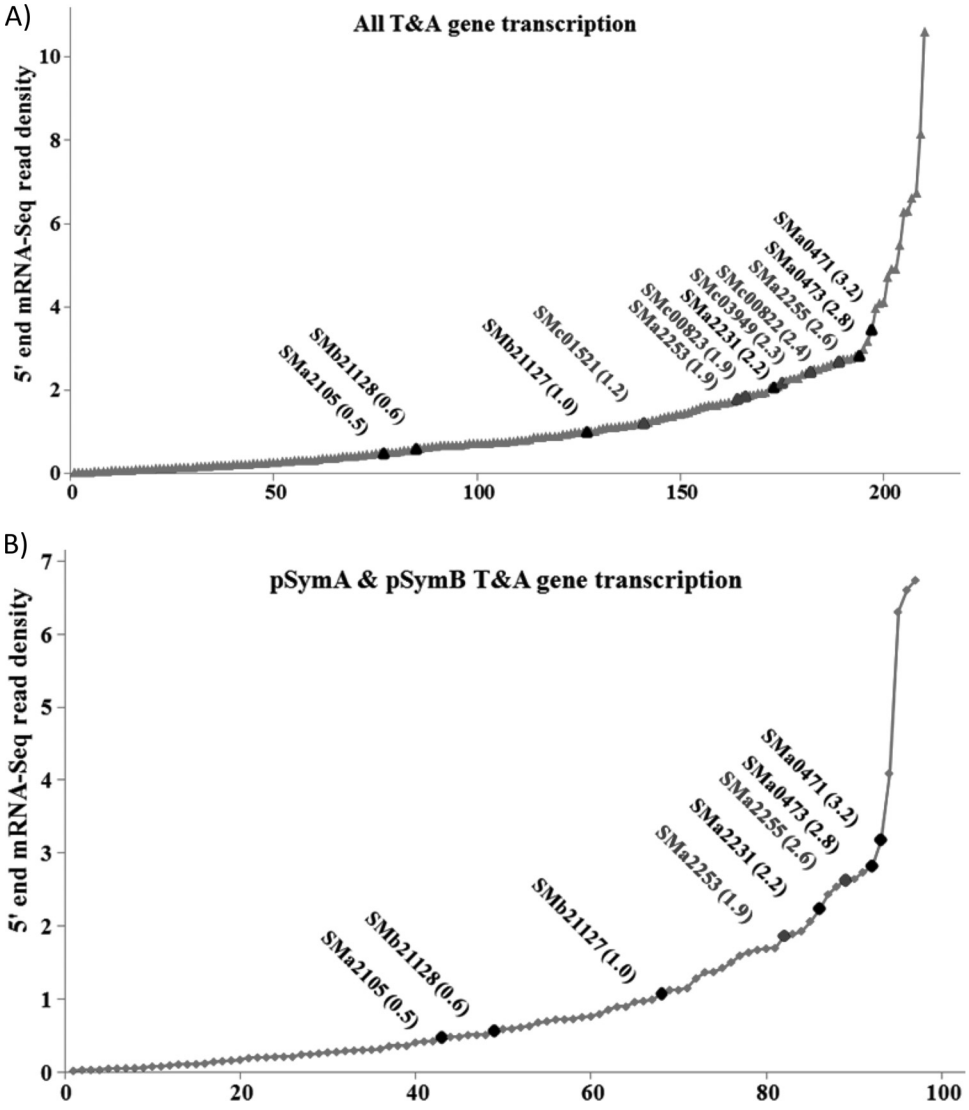

FIG 7 Rank order expression of TA-associated genes from the whole *S. meliloti* genome (A) and the pSymA and pSymB megaplasmids of *S. meliloti* (B). RNA-seq read data were the mean data obtained using mRNA from *S. meliloti* P110 cells grown in media with limiting and excess phosphate. Those RNA-seq counts were combined with RNA-seq data extracted from Rm2011 cells as outlined by Sallet et al. (41). The expression was quantified as frequency of 5′ RNA-seq read counts per nucleotide within a given gene region, and the *x* axis represents the order of TA genes from the least to the most highly expressed. The expression data for each gene are in Table S3 in the supplemental material.

ogy and metabolism and grew slowly in rich medium (61). Dusha and coworkers also characterized a *vapBC*-like locus, *ntrPR*, in *S. meliloti*, which appears to be involved in the regulation of symbiotic nitrogen fixation. Deletion of the locus improves the symbiotic phenotype of *S. meliloti* (62–64). Mutations within *ntrR* also resulted in a pleiotropic effect, with a total of 440 transcripts showing differential abundance compared to the wild type under either aerobic or microaerobic conditions (63). In wild-type bacteria, large-scale transcriptomic changes occur during symbiosis, and the potential for these to be regulated through the activity of TA systems is intriguing (64). Other studies have suggested that TA systems are involved in the selective expression of a subset of genes during developmental processes such as biofilm formation, sporulation, and pathogenesis (65–67). Dry weight measurements of alfalfa plants inoculated with the *S. meliloti* deletion strains that lack each of the four TA loci identified here were indistinguishable from those of plants inoculated with the wild type (data not shown). Hence, these TA systems did not appear to have any effect on symbiotic N_2 fixation with alfalfa. However, further studies are necessary to investigate whether the TA systems might play a role in the bacteroid death process that accompanies nodule senescence.

Here, we have focused on the use of the megaplasmid deletion strains in the identification of active toxin-antitoxin loci; however, this strain collection is a valuable tool for studies looking to unravel how these megaplasmids contribute to the biology of the cell. This strain collection has previously been employed in the identification of essential genes, a cobalt transport system, and a hydroxyproline transport and metabolic gene cluster (29, 42, 68). The availability of this strain collection will aid researchers in future studies examining the contributions of pSymA and pSymB to both free-living and symbiotic *S. meliloti* cells.

ACKNOWLEDGMENTS

This work was supported by grants to T.M.F. from the Natural Sciences and Engineering Research Council of Canada. T.M.F. also acknowledges support from Genome Canada, OGI, and the Ontario Research and Development Challenge Fund.

We are very grateful to Marie Elliot and Ye Zhang for insights, interest, and advice and Erika Sallet for clarifications regarding the Rm2011 RNA-seq data.

REFERENCES

1. **Makarova KS, Wolf YI, Koonin EV.** 2009. Comprehensive comparative-genomic analysis of type 2 toxin-antitoxin systems and related mobile stress response systems in prokaryotes. Biol. Direct **4:**19. http://dx.doi.org/10.1186/1745-6150-4-19.
2. **Yamaguchi Y, Park JH, Inouye M.** 2011. Toxin-antitoxin systems in bacteria and archaea. Annu. Rev. Genet. **45:**61–79. http://dx.doi.org/10.1146/annurev-genet-110410-132412.
3. **Syed MA, Levesque CM.** 2012. Chromosomal bacterial type II toxin-antitoxin systems. Can. J. Microbiol. **58:**553–562. http://dx.doi.org/10.1139/w2012-025.
4. **Yarmolinsky MB.** 1995. Programmed cell death in bacterial populations. Science **267:**836–837. http://dx.doi.org/10.1126/science.7846528.
5. **Lehnherr H, Maguin E, Jafri S, Yarmolinsky MB.** 1993. Plasmid addiction genes of bacteriophage P1: Doc, which causes cell death on curing of prophage, and *phd*, which prevents host death when prophage is retained. J. Mol. Biol. **233:**414–428. http://dx.doi.org/10.1006/jmbi.1993.1521.
6. **Christensen SK, Maenhaut-Michel G, Mine N, Gottesman S, Gerdes K, Van Melderen L.** 2004. Overproduction of the *lon* protease triggers inhibition of translation in *Escherichia coli*: involvement of the *yefM-yoeB* toxin-antitoxin system. Mol. Microbiol. **51:**1705–1717. http://dx.doi.org/10.1046/j.1365-2958.2003.03941.x.
7. **Schuster CF, Bertram R.** 2013. Toxin-antitoxin systems are ubiquitous and versatile modulators of prokaryotic cell fate. FEMS Microbiol. Lett. **340:**73–85. http://dx.doi.org/10.1111/1574-6968.12074.
8. **Jiang Y, Pogliano J, Helinski DR, Konieczny I.** 2002. ParE toxin encoded by the broad-host-range plasmid RK2 is an inhibitor of *Escherichia coli* gyrase. Mol. Microbiol. **44:**971–979. http://dx.doi.org/10.1046/j.1365-2958.2002.02921.x.
9. **Zhang Y, Zhang J, Hara H, Kato I, Inouye M.** 2005. Insights into the mRNA cleavage mechanism by MazF, an mRNA interferase. J. Biol. Chem. **280:**3143–3150. http://dx.doi.org/10.1074/jbc.M411811200.
10. **Liu M, Zhang Y, Inouye M, Woychik NA.** 2008. Bacterial addiction module toxin *doc* inhibits translation elongation through its association with the 30S ribosomal subunit. Proc. Natl. Acad. Sci. U. S. A. **105:**5885–5890. http://dx.doi.org/10.1073/pnas.0711949105.
11. **Van Melderen L, Saavedra De Bast M.** 2009. Bacterial toxin-antitoxin systems: more than selfish entities? PLoS Genet. **5:**e1000437. http://dx.doi.org/10.1371/journal.pgen.1000437.
12. **Gerdes K, Rasmussen PB, Molin S.** 1986. Unique type of plasmid maintenance function: postsegregational killing of plasmid-free cells. Proc. Natl. Acad. Sci. U. S. A. **83:**3116–3120. http://dx.doi.org/10.1073/pnas.83.10.3116.
13. **Saavedra De Bast M, Mine N, Van Melderen L.** 2008. Chromosomal toxin-antitoxin systems may act as antiaddiction modules. J. Bacteriol. **190:**4603–4609. http://dx.doi.org/10.1128/JB.00357-08.
14. **Fineran PC, Blower TR, Foulds IJ, Humphreys DP, Lilley KS, Salmond GP.** 2009. The phage abortive infection system, ToxIN, functions as a protein-RNA toxin-antitoxin pair. Proc. Natl. Acad. Sci. U. S. A. **106:**894–899. http://dx.doi.org/10.1073/pnas.0808832106.
15. **Aizenman E, Engelberg-Kulka H, Glaser G.** 1996. An *Escherichia coli* chromosomal "addiction module" regulated by guanosine 3′,5′-bispyrophosphate: a model for programmed bacterial cell death. Proc. Natl. Acad. Sci. U. S. A. **93:**6059–6063. http://dx.doi.org/10.1073/pnas.93.12.6059.
16. **Christensen SK, Mikkelsen M, Pedersen K, Gerdes K.** 2001. RelE, a global inhibitor of translation, is activated during nutritional stress. Proc. Natl. Acad. Sci. U. S. A. **98:**14328–14333. http://dx.doi.org/10.1073/pnas.251327898.
17. **Dorr T, Vulic M, Lewis K.** 2010. Ciprofloxacin causes persister formation by inducing the TisB toxin in *Escherichia coli*. PLoS Biol. **8:**e1000317. http://dx.doi.org/10.1371/journal.pbio.1000317.
18. **Galibert F, Finan TM, Long SR, Puhler A, Abola P, Ampe F, Barloy-Hubler F, Barnett MJ, Becker A, Boistard P, Bothe G, Boutry M, Bowser L, Buhrmester J, Cadieu E, Capela D, Chain P, Cowie A, Davis RW, Dréano S, Federspiel NA, Fisher RF, Gloux S, Godrie T, Goffeau A, Golding B, Gouzy J, Gurjal M, Hernandez-Lucas I, Hong A, Huizar L, Hyman RW, Jones T, Kahn D, Kahn ML, Kalman S, Keating DH, Kiss E, Komp C, Lelaure V, Masuy D, Palm C, Peck MC, Pohl TM, Portetelle D, Purnelle B, Ramsperger U, Surzycki R, Thébault P, Vandenbol M, Vorhölter F-J, Weidner S, Wells DH, Wong K, Yeh K-C, Batut J.** 2001. The composite genome of the legume symbiont *Sinorhizobium meliloti*. Science **293:**668–672. http://dx.doi.org/10.1126/science.1060966.
19. **Barnett MJ, Fisher RF, Jones T, Komp C, Abola AP, Barloy-Hubler F, Bowser L, Capela D, Galibert F, Gouzy J, Gurjal M, Hong A, Huizar L, Hyman RW, Kahn D, Kahn ML, Kalman S, Keating DH, Palm C, Peck MC, Surzycki R, Wells DH, Yeh KC, Davis RW, Federspiel NA, Long SR.** 2001. Nucleotide sequence and predicted functions of the entire *Sinorhizobium meliloti* pSymA megaplasmid. Proc. Natl. Acad. Sci. U. S. A. **98:**9883–9888. http://dx.doi.org/10.1073/pnas.161294798.
20. **Finan TM, Weidner S, Wong K, Buhrmester J, Chain P, Vorhölter FJ, Hernandez-Lucas I, Becker A, Cowie A, Gouzy J, Golding B, Pühler A.** 2001. The complete sequence of the 1,683-kb pSymB megaplasmid from the N2-fixing endosymbiont *Sinorhizobium meliloti*. Proc. Natl. Acad. Sci. U. S. A. **98:**9889–9894. http://dx.doi.org/10.1073/pnas.161294698.
21. **Banfalvi Z, Sakanyan V, Koncz C, Kiss A, Dusha I, Kondorosi A.** 1981. Location of nodulation and nitrogen fixation genes on a high molecular weight plasmid of *R. meliloti*. Mol. Gen. Genet. **184:**318–325.
22. **Hynes MF, Simon R, Müller P, Niehaus K, Labes M, Pühler A.** 1986. The two megaplasmids of *Rhizobium meliloti* are involved in the effective nodulation of alfalfa. Mol. Gen. Genet. **202:**356–362. http://dx.doi.org/10.1007/BF00333262.
23. **Finan TM, Kunkel B, De Vos GF, Signer ER.** 1986. Second symbiotic megaplasmid in *Rhizobium meliloti* carrying exopolysaccharide and thiamine synthesis genes. J. Bacteriol. **167:**66–72.
24. **Holloway P, McCormick W, Watson RJ, Chan YK.** 1996. Identification and analysis of the dissimilatory nitrous oxide reduction genes, *nosRZDFY*, of *Rhizobium meliloti*. J. Bacteriol. **178:**1505–1514.
25. **Torres MJ, Rubia MI, Bedmar EJ, Delgado MJ.** 2011. Denitrification in *Sinorhizobium meliloti*. Biochem. Soc. Trans. **39:**1886–1889. http://dx.doi.org/10.1042/BST20110733.
26. **Mauchline TH, Fowler JE, East AK, Sartor AL, Zaheer R, Hosie AHF, Poole PS, Finan TM.** 2006. Mapping the *Sinorhizobium meliloti* 1021 solute-binding protein-dependent transportome. Proc. Natl. Acad. Sci. U. S. A. **103:**17933–17938. http://dx.doi.org/10.1073/pnas.0606673103.
27. **Biondi EG, Tatti E, Comparini D, Giuntini E, Mocali S, Giovannetti L, Bazzicalupo M, Mengoni A, Viti C.** 2009. Metabolic capacity of *Sinorhizobium* (ensifer) *meliloti* strains as determined by phenotype MicroArray analysis. Appl. Environ. Microbiol. **75:**5396–5404. http://dx.doi.org/10.1128/AEM.00196-09.
28. **Dominguez-Ferreras A, Perez-Arnedo R, Becker A, Olivares J, Soto MJ, Sanjuan J.** 2006. Transcriptome profiling reveals the importance of plasmid pSymB for osmoadaptation of *Sinorhizobium meliloti*. J. Bacteriol. **188:**7617–7625. http://dx.doi.org/10.1128/JB.00719-06.
29. **diCenzo G, Milunovic B, Cheng J, Finan TM.** 2013. The tRNAarg gene and *engA* are essential genes on the 1.7-mb pSymB megaplasmid of *Sinorhizobium meliloti* and were translocated together from the chromosome in an ancestral strain. J. Bacteriol. **195:**202–212. http://dx.doi.org/10.1128/JB.01758-12.
30. **Oresnik IJ, Liu SL, Yost CK, Hynes MF.** 2000. Megaplasmid pRme2011a of *Sinorhizobium meliloti* is not required for viability. J. Bacteriol. **182:**3582–3586. http://dx.doi.org/10.1128/JB.182.12.3582-3586.2000.
31. **Yurgel SN, Mortimer MW, Rice JT, Humann JL, Kahn ML.** 2013. Directed construction and analysis of a *Sinorhizobium meliloti* pSymA deletion mutant library. Appl. Environ. Microbiol. **79:**2081–2087. http://dx.doi.org/10.1128/AEM.02974-12.
32. **Sevin EW, Barloy-Hubler F.** 2007. RASTA-Bacteria: a web-based tool for identifying toxin-antitoxin loci in prokaryotes. Genome Biol. **8:**R155. http://dx.doi.org/10.1186/gb-2007-8-8-r155.
33. **Yuan ZC, Zaheer R, Finan TM.** 2006. Regulation and properties of PstSCAB, a high-affinity, high-velocity phosphate transport system of *Sinorhizobium meliloti*. J. Bacteriol. **188:**1089–1102. http://dx.doi.org/10.1128/JB.188.3.1089-1102.2006.
34. **Charles TC, Finan TM.** 1991. Analysis of a 1600-kilobase *Rhizobium*

meliloti megaplasmid using defined deletions generated in vivo. Genetics **127:**5–20.
35. **Cowie A, Cheng J, Sibley CD, Fong Y, Zaheer R, Patten CL, Morton RM, Golding GB, Finan TM.** 2006. An integrated approach to functional genomics: construction of a novel reporter gene fusion library for *Sinorhizobium meliloti*. Appl. Environ. Microbiol. **72:**7156–7167. http://dx.doi.org/10.1128/AEM.01397-06.
36. **Sambrook J, Fritsch EF, Maniatis T.** 1989. Molecular cloning: a laboratory manual, 2nd ed. Cold Spring Harbor Laboratory Press, Cold Spring Harbor, NY.
37. **Chang AC, Cohen SN.** 1978. Construction and characterization of amplifiable multicopy DNA cloning vehicles derived from the P15A cryptic miniplasmid. J. Bacteriol. **134:**1141–1156.
38. **Snaith MR, Murray JA, Boulter CA.** 1995. Multiple cloning sites carrying loxP and FRT recognition sites for the *cre* and *flp* site-specific recombinases. Gene **166:**173–174. http://dx.doi.org/10.1016/0378-1119(95)00579-8.
39. **Korch SB, Contreras H, Clark-Curtiss JE.** 2009. Three *Mycobacterium tuberculosis rel* toxin-antitoxin modules inhibit *Mycobacterial* growth and are expressed in infected human macrophages. J. Bacteriol. **191:**1618–1630. http://dx.doi.org/10.1128/JB.01318-08.
40. **Chain PSG.** 1998. Development of an *in vivo* DNA cloning procedure for bacteria. M.Sc thesis. McMaster University, Hamilton, Ontario, Canada.
41. **Sallet E, Roux B, Sauviac L, Jardinaud MF, Carrere S, Faraut T, de Carvalho-Niebel F, Gouzy J, Gamas P, Capela D, Bruand C, Schiex T.** 2013. Next-generation annotation of prokaryotic genomes with EuGene-P: application to *Sinorhizobium meliloti* 2011. DNA Res. **20:**339–354. http://dx.doi.org/10.1093/dnares/dst014.
42. **Cheng J, Poduska B, Morton RA, Finan TM.** 2011. An ABC-type cobalt transport system is essential for growth of *Sinorhizobium meliloti* at trace metal concentrations. J. Bacteriol. **193:**4405–4416. http://dx.doi.org/10.1128/JB.05045-11.
43. **Gerdes K.** 2013. Type II toxin-antitoxin loci: the *relBE* family, p 69–92. *In* Gerdes K (ed), Prokaryotic toxin-antitoxins. Springer, Berlin, Germany.
44. **Neubauer C, Gao YG, Andersen KR, Dunham CM, Kelley AC, Hentschel J, Gerdes K, Ramakrishnan V, Brodersen DE.** 2009. The structural basis for mRNA recognition and cleavage by the ribosome-dependent endonuclease RelE. Cell **139:**1084–1095. http://dx.doi.org/10.1016/j.cell.2009.11.015.
45. **Goeders N, Dreze PL, Van Melderen L.** 2013. Relaxed cleavage specificity within the RelE toxin family. J. Bacteriol. **195:**2541–2549. http://dx.doi.org/10.1128/JB.02266-12.
46. **Christensen SK, Gerdes K.** 2003. RelE toxins from bacteria and archaea cleave mRNAs on translating ribosomes, which are rescued by tmRNA. Mol. Microbiol. **48:**1389–1400. http://dx.doi.org/10.1046/j.1365-2958.2003.03512.x.
47. **Nieto C, Pellicer T, Balsa D, Christensen SK, Gerdes K, Espinosa M.** 2006. The chromosomal *relBE2* toxin-antitoxin locus of *Streptococcus pneumoniae*: characterization and use of a bioluminescence resonance energy transfer assay to detect toxin-antitoxin interaction. Mol. Microbiol. **59:**1280–1296. http://dx.doi.org/10.1111/j.1365-2958.2006.05027.x.
48. **Garcio-Pino A, Sterckx Y, Magnuson RD, Loris R.** 2013. Type II toxin-antitoxin loci: the *phd*/*doc* family, p 157–176. *In* Gerdes K (ed), Prokaryotic toxin-antitoxins. Springer, Berlin, Germany.
49. **Garcia-Pino A, Christensen-Dalsgaard M, Wyns L, Yarmolinsky M, Magnuson RD, Gerdes K, Loris R.** 2008. Doc of prophage P1 is inhibited by its antitoxin partner *phd* through fold complementation. J. Biol. Chem. **283:**30821–30827. http://dx.doi.org/10.1074/jbc.M805654200.
50. **Arcus VL, McKenzie JL, Robson J, Cook GM.** 2011. The PIN-domain ribonucleases and the prokaryotic VapBC toxin-antitoxin array. Protein Eng. Des. Sel. **24:**33–40. http://dx.doi.org/10.1093/protein/gzq081.
51. **Ramage HR, Connolly LE, Cox JS.** 2009. Comprehensive functional analysis of *Mycobacterium tuberculosis* toxin-antitoxin systems: implications for pathogenesis, stress responses, and evolution. PLoS Genet. **5:**e1000767. http://dx.doi.org/10.1371/journal.pgen.1000767.
52. **Robson J, McKenzie JL, Cursons R, Cook GM, Arcus VL.** 2009. The *vapBC* operon from *Mycobacterium smegmatis* is an autoregulated toxin-antitoxin module that controls growth via inhibition of translation. J. Mol. Biol. **390:**353–367. http://dx.doi.org/10.1016/j.jmb.2009.05.006.
53. **Winther KS, Gerdes K.** 2011. Enteric virulence associated protein VapC inhibits translation by cleavage of initiator tRNA. Proc. Natl. Acad. Sci. U. S. A. **108:**7403–7407. http://dx.doi.org/10.1073/pnas.1019587108.
54. **Finn RD, Tate J, Mistry J, Coggill PC, Sammut SJ, Hotz HR, Ceric G, Forslund K, Eddy SR, Sonnhammer EL, Bateman A.** 2008. The Pfam protein families database. Nucleic Acids Res. **36:**D281–D288. http://dx.doi.org/10.1093/nar/gkm960.
55. **Wood HE, Devine KM, McConnell DJ.** 1990. Characterisation of a repressor gene (*xre*) and a temperature-sensitive allele from the *Bacillus subtilis* prophage, PBSX. Gene **96:**83–88. http://dx.doi.org/10.1016/0378-1119(90)90344-Q.
56. **Mine N, Guglielmini J, Wilbaux M, Van Melderen L.** 2009. The decay of the chromosomally encoded *ccdO157* toxin-antitoxin system in the *Escherichia coli* species. Genetics **181:**1557–1566. http://dx.doi.org/10.1534/genetics.108.095190.
57. **Wilbaux M, Mine N, Guerout AM, Mazel D, Van Melderen L.** 2007. Functional interactions between coexisting toxin-antitoxin systems of the *ccd* family in *Escherichia coli* O157:H7. J. Bacteriol. **189:**2712–2719. http://dx.doi.org/10.1128/JB.01679-06.
58. **Fiebig A, Castro Rojas CM, Siegal-Gaskins D, Crosson S.** 2010. Interaction specificity, toxicity and regulation of a paralogous set of ParE/RelE-family toxin-antitoxin systems. Mol. Microbiol. **77:**236–251. http://dx.doi.org/10.1111/j.1365-2958.2010.07207.x.
59. **Yang M, Gao C, Wang Y, Zhang H, He ZG.** 2010. Characterization of the interaction and cross-regulation of three *Mycobacterium tuberculosis* RelBE modules. PLoS One **5:**e10672. http://dx.doi.org/10.1371/journal.pone.0010672.
60. **Smith AB, Lopez-Villarejo J, Diago-Navarro E, Mitchenall LA, Barendregt A, Heck AJ, Lemonnier M, Maxwell A, Diaz-Orejas R.** 2012. A common origin for the bacterial toxin-antitoxin systems *parD* and *ccd*, suggested by analyses of toxin/target and toxin/antitoxin interactions. PLoS One **7:**e46499. http://dx.doi.org/10.1371/journal.pone.0046499.
61. **Miclea PS, Peter M, Vegh G, Cinege G, Kiss E, Varo G, Horvath I, Dusha I.** 2010. Atypical transcriptional regulation and role of a new toxin-antitoxin-like module and its effect on the lipid composition of *Bradyrhizobium japonicum*. Mol. Plant Microbe Interact. **23:**638–650. http://dx.doi.org/10.1094/MPMI-23-5-0638.
62. **Olah B, Kiss E, Gyorgypal Z, Borzi J, Cinege G, Csanadi G, Batut J, Kondorosi A, Dusha I.** 2001. Mutation in the *ntrR* gene, a member of the *vap* gene family, increases the symbiotic efficiency of *Sinorhizobium meliloti*. Mol. Plant Microbe Interact. **14:**887–894. http://dx.doi.org/10.1094/MPMI.2001.14.7.887.
63. **Puskas LG, Nagy ZB, Kelemen JZ, Ruberg S, Bodogai M, Becker A, Dusha I.** 2004. Wide-range transcriptional modulating effect of *ntrR* under microaerobiosis in *Sinorhizobium meliloti*. Mol. Genet. Genomics **272:**275–289. http://dx.doi.org/10.1007/s00438-004-1051-3.
64. **Capela D, Filipe C, Bobik C, Batut J, Bruand C.** 2006. *Sinorhizobium meliloti* differentiation during symbiosis with alfalfa: a transcriptomic dissection. Mol. Plant Microbe Interact. **19:**363–372. http://dx.doi.org/10.1094/MPMI-19-0363.
65. **Nariya H, Inouye M.** 2008. MazF, an mRNA interferase, mediates programmed cell death during multicellular *Myxococcus* development. Cell **132:**55–66. http://dx.doi.org/10.1016/j.cell.2007.11.044.
66. **Zhu L, Phadtare S, Nariya H, Ouyang M, Husson RN, Inouye M.** 2008. The mRNA interferases, MazF-mt3 and MazF-mt7 from *Mycobacterium tuberculosis* target unique pentad sequences in single-stranded RNA. Mol. Microbiol. **69:**559–569. http://dx.doi.org/10.1111/j.1365-2958.2008.06284.x.
67. **Yamaguchi Y, Park JH, Inouye M.** 2009. MqsR, a crucial regulator for quorum sensing and biofilm formation, is a GCU-specific mRNA interferase in *Escherichia coli*. J. Biol. Chem. **284:**28746–28753. http://dx.doi.org/10.1074/jbc.M109.032904.
68. **Maclean AM, White CE, Fowler JE, Finan TM.** 2009. Identification of a hydroxyproline transport system in the legume endosymbiont *Sinorhizobium meliloti*. Mol. Plant Microbe Interact. **22:**1116–1127. http://dx.doi.org/10.1094/MPMI-22-9-1116.